Acta Mechanica Slovaca **28 (3): 26 - 34,** September **2024**
https://doi.org/10.21496/ams.2024.012

Acta Mechanica Slovaca
ISSN 1335-2393
www.actamechanica.sk

Theoretical and Numerical Study on the Dynamic Behaviour of a Rotor with a Conical Steel Shaft

Rachid Zahi [1,*] , Habib Achache [2]

[1] Relizane University Algeria
[2] Institute of maintenance and industrial safety, University of Oran2 Mohamed Ben Ahmed, B.P 1015 El M'naouer 31000 Oran, Algeria, Laboratory of Physical Mechanics of Materials Sidi Bel Abbes, Algeria

Abstract: This work proposes a theoretical and numerical study on the behaviour of the tapered rotor. The characteristics of the elements of the rotor are determined; it is to evaluate the expressions of the kinetic and potential energies as well as the virtual work corresponding to the basic elements disk, shaft, bearing for the two conical models by applying the method of the finite elements. Numerical simulation allows us to observe and determine modal analysis and natural values.

Keywords: Finite element method; tapered rotor; vibration; dynamic behaviour.

Nomenclature :

- ω = *Angular velocity of the rotor (rad/s)*
- ζ = *Damping ratio (dimensionless)*
- κ = *Stiffness of the rotor shaft (N/m)*
- c = *Damping coefficient (N·s/m)*
- m = *Mass of the rotor (kg)*
- ϕ = *Deflection angle (rad)*
- E = *Modulus of elasticity of the shaft material (Pa)*
- I = *Area moment of inertia of the shaft cross-section (m44)*
- L = *Length of the shaft (m)*
- fn = *Natural frequency (Hz)*
- τ = *Torsional stiffness (Nm/rad)*
- δ = *Displacement (m)*

Abbreviations

- *FEM = Finite Element Method*
- *RPM = Revolutions Per Minute*
- *FE = Finite Element*
- *BVP = Boundary Value Problem*
- *SDOF = Single Degree of Freedom*

Indices

- *i,j = Node indices in finite element analysis*
- *n = Mode number in vibration analysis*

Units

- *[rad/s] = Radians per second*
- *[N/m] = Newton per meter*
- *[N·s/m] = Newton second per meter*
- *[kg] = Kilogram*
- *[rad] = Radian*
- *[Pa] = Pascal*
- *[m^3] = Cubic meters*
- *[m] = Meter*

*** Corresponding author:** Rachid Zahi, ***E-mail address:*** *zahirachid72@yahoo.fr*

– *[Hz] = Hertz*
– *[Nm/rad] = Newton meter per radian*
– *[m] = Meter*

1. Introduction

In various industrial applications, the rotor-bearing system plays a critical role in ensuring the smooth operation and performance of turbomachinery, power plants, machine tools, automobiles, household appliances, and aerospace systems. This system is subject to complex dynamic behaviors influenced by factors such as rotational inertia, axial loads, gyroscopic effects, unbalanced masses, and nonlinear forces induced by fluid films.

Nelson and McVaugh pioneered the development of finite element models for rotor-bearing systems, utilizing C1 type cylindrical finite elements with four degrees of freedom per nodal point, incorporating both transverse displacements and rotations [1]. This approach accounted for essential factors such as rotational inertia, axial loads, and gyroscopic forces. Subsequent advancements by Gash and Zorzi et al. extended this modeling to include internal damping effects [2,3]. Nelson further refined the finite element model based on Timoshenko's beam theory, which was subsequently enhanced by Ôzgtuven and Ozkan [5]. The effectiveness of these techniques was validated through subsequent works, confirming their reliability and maturity [6-8].

Further advancements introduced linearly conical elements based on Timoshenko's beam theory, incorporating shear effects through additional nodal variables, resulting in twelve degrees of freedom per element [9]. Greenhill et al. extended this approach to encompass all intrinsic rotational effects in a conical element formulation, providing closed-form expressions for elementary structural matrices.

The dynamic behavior of rotor-bearing systems is significantly influenced by unbalanced masses in rotating discs and nonlinear forces induced by fluid films. Jia et al. developed a non-probabilistic convex model using the Chebyshev Convex Method (CCM) to characterize uncertain parameters in Jeffcott rotor systems [10]. Numanoğlu et al. emphasized the importance of nonlocal finite element methods for analyzing the vibration behavior of nanobeams [11]. Ahmed et al. studied elastic Jeffcott rotors using a finite element model and small disturbance method, revealing the significant impact of rotational speed changes on rotor stability [12].

Ghayesh et al. conducted analytical studies on parametric and forced nonlinear vibrations of axially moving rotors [13]. Jeong demonstrated the efficacy of model order reduction for large-scale rotor-dynamic systems using Krylov subspace-based finite element discretization, accelerating analyses while maintaining accuracy [14]. Fatehi et al. proposed a novel approach to increase the convergence speed of Sobol indices, enhancing global sensitivity analysis [15]. Saldarriaga et al. proposed an experimental methodology to balance highly flexible nonlinear rotors using neural networks [16].

Liu et al. provided a comprehensive overview of drone developments and their applications in civil engineering, covering hardware, software, control methodologies, and potential applications [17]. Muñoz-Abella et al. presented a methodology for crack identification in unbalanced rotors using artificial neural networks [18]. Matthew et al. proposed a double screw positive displacement machine configuration, analyzing rotor geometry effects [19]. Vinod et al. performed dynamic analysis of a 3D FE rotor-shaft system, validating results against experimental data [20]. Shravankumar et al. conducted numerical analysis of a rotor shaft system to prevent vibration [21], and Gayen et al. numerically analyzed a functionally graded shaft system in thermal environments [22].

"Genta and Gugliotta (1988) introduced a conical element for finite element rotor dynamics in their work published in the Journal of Sound and Vibration [23]. Additionally, Rachid et al. (2023) conducted a dynamic analysis of a rotating tapered composite Timoshenko shaft, as reported in Steel and Composite Structures. Furthermore, Zahi et al. (2023) investigated the study and analysis of a tapered shaft in composite materials with variable speed of rotation, as published in Structural Engineering and Mechanics [24, 25].

In the present work, a finite element formulation was developed for vibration analysis of a rotor with conical shafts. The study included transverse shear deformation theory, rotational inertia, and gyroscopic effects. A dedicated program was developed to calculate natural frequencies and critical speeds, with results rigorously compared to existing literature, showcasing advancements and

ensuring reliability in rotor-bearing system analysis.

2. Cinematic Equations

The Figure 1 shows a circular or annular conical beam with a linearly variable thickness. The expression for sector A and the diametric and polar moments of the inertia Id and Ip of the section are:

$$A(\zeta) = A_j\left(1+\alpha_1\zeta+\beta_1\zeta\right) \tag{1}$$

$$I_d(\zeta) = I_{dj}\left(1+\alpha_2\zeta+\beta_2\zeta^2+\gamma_3\zeta^3+\delta_2\zeta^4\right) \tag{2}$$

$$I_p = 2I_d$$

The non-dimensional coordinated is:

$$\zeta = z/l \tag{3}$$

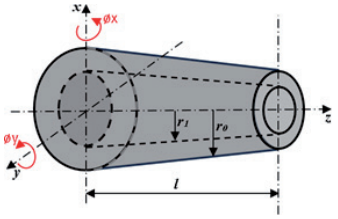

Figure 1: The tapered element [23].

The expressions for the geometric coefficients in equations (2) and (3) are:

$$\left\{\begin{matrix}\left[n_1\right]=\left[1/(1+\phi)\right]\left[\begin{matrix}1+\phi(1-\zeta)-3\zeta^3+2\zeta^3;1\zeta\left[1+\frac{1}{2}\phi(1-\zeta)-2\zeta+\zeta^2\right];\\ \zeta\left(3\zeta-2\zeta^2+\phi\right);l\zeta\left[-\frac{1}{2}\phi(1-\zeta)-2\zeta+\zeta^2\right]\end{matrix}\right]\\ \left[n_2\right]=\left[1/(1+\phi)\right]\left[6\zeta(\zeta-1);l\left[1-4\zeta+3\zeta^3+\phi(1-\zeta)\right];-6\zeta(\zeta-1);l\left[-2\zeta+3\zeta^2+\phi\zeta\right]\right]\end{matrix}\right\} \tag{8}$$

The value of the constant $\phi = 12EI_d\chi/gAl^2$ can be calculated by using the geometric properties A, I, and the section in the middle of the element. The matrices: stiffness [K], mass [m], gyroscopic [G], structural damping [k"], and geometric matrix (axial forces) [kg] are defined as:

$$[K] = \frac{E}{l}\int_0^1 I_d\left(\frac{d}{d\zeta}[n_2]^T\frac{d}{d\zeta}[n_2]\right)d\zeta + gl\int_0^1\frac{A}{\chi}\left[[n_2]-\frac{d}{d\zeta}[n_1]\right]^T\left[[n_2]-\frac{d}{d\zeta}[n_1]\right]d\zeta \tag{9}$$

$$[m] = [m_T]+[m_R] = pl\left(\int_0^1 A[n_1]^T[n_1]d\zeta+\int_0^1 I_d[n_2]^T[n_2]d\zeta\right) \tag{10}$$

$$[G] = pl\int_0^1 I_p[n_2]^T[n_2]d\zeta = 2[m_R] \tag{11}$$

$$[k''] = \eta[K] \tag{12}$$

$$[k_g] = \frac{F_a}{l}\int_0^1\frac{d}{d\zeta}[n_1]^T\frac{d}{d\zeta}[n_1]d\zeta \tag{13}$$

$$\left\{\begin{matrix}\alpha_1 = 2\pi\left(r_{0j}\Delta r_0 - r_{ij}\Delta r_i\right)/A_j, & \beta_1 = \pi\left(\Delta r_0^2-\Delta r_i^2\right)/A_j\\ \alpha_2 = \pi\left(r_{0j}^3\Delta r_0 - r_{ij}^3\Delta r_i\right)/I_{dj}, & \beta_2 = 3\pi\left(r_{0j}^2\Delta r_0^2 - r_{ij}^2\Delta r_i^2\right)/2I_{dj}\\ \gamma_2 = \pi\left(r_{0j}\Delta r_0^3 - r_{ij}\Delta r_i^3\right)/I_{dj}, & \delta_2 = \pi\left(\Delta r_0^4-\Delta r_i^2\right)/4I_{dj}\end{matrix}\right\} \tag{4}$$

Withe:

$$\Delta r_0 = r_{0k}-r_{0j}, \quad \Delta r_i = r_{ik}-r_{ij} \tag{5}$$

3. Element Matrix

The displacements of the beam can be expressed, in complex notation, as follows:

$$\left\{\bar{z}\right\} = \begin{Bmatrix}x+i\cdot y\\ \phi_y - i\cdot\phi_y\end{Bmatrix} = \begin{bmatrix}n_1\\ n_2\end{bmatrix}\left\{\bar{q}\right\} \tag{6}$$

The vector {q} enumerating the generalized complex coordinates:

$$\left\{\bar{q}\right\}^T = \left[x_j,\phi_{yj},x_k,\phi_{yk}\right]+i\left[y_i,-\phi_{xj},y_k,-\phi_{xk}\right] \tag{7}$$

The shape functions [n1] and [n2] are based on the usual formulation for a Timoshenko beam element.

The expressions for the matrices of the conic element are:

$$[K]=\frac{EI_j}{10l^3(1+\phi)^2}\begin{bmatrix} k_1 & lk_2 & -k_1 & lk_3 \\ & l^2k_4 & -lk_2 & l^2k_5 \\ & & k_1 & -lk_3 \\ symm & & & l^2k_6 \end{bmatrix}+\frac{gA_j\phi^2}{12\chi l(1+\phi)^2}\begin{bmatrix} k_7 & lk_8 & -k_7 & lk_8 \\ & l^2k_9 & -lk_8 & l^2k_9 \\ & & k_7 & -lk_8 \\ symm & & & l^2k_9 \end{bmatrix} \tag{14}$$

$$k_4=420+210\phi+105\phi^2+\alpha_2(105+52.5\phi^2)+\beta_2(56-35\phi+35\phi^2)+\gamma_2(42-42\phi+26.25\phi^2)+\delta_2(36-42\phi+21\phi^2)$$

$$k_5=210+210\phi+105\phi^2+\alpha_2(105+105\phi^2-52.5\phi^2)+\beta_2(91-70\phi-35\phi^2)+\gamma_2(84-52.5\phi-26.25\phi^2)+\delta_2(78-42\phi+21\phi^2)$$

$$k_6=420+210\phi+105\phi^2+\alpha_2(315-210\phi-52.5\phi^2)+\beta_2(266-175\phi+35\phi^2)+\gamma_2(231-147\phi-26.25\phi^2)+\delta_2(204-126\phi+21\phi^2)$$

$$k_7=(12+6\alpha_1+4\beta_1)$$

$$k_8=(6+3\alpha_1+2\beta_1)$$

$$k_9=(3+1.5\alpha_1+\beta_1)$$

$$[m_T]=\frac{\rho A_j l}{1260(1+\phi)^2}\begin{bmatrix} m_1 & lm_2 & m_3 & -lm_4 \\ & l^2m_5 & lm_6 & -l^2m_7 \\ & & m_8 & -lm_9 \\ symm & & & l^2m_{10} \end{bmatrix} \tag{15}$$

Where:

$$m_1=(468+882\phi+420\phi^2)+\alpha_1(108+210\phi+105\phi^2)+\beta_1(38+78\phi+42\phi^2)$$

$$m_2=(66+115.5\phi+52.5\phi^2)+\alpha_1(21+40.5\phi+21\phi^2)+\beta_1(8.5+18\phi+10.5\phi^2)$$

$$m_3=(162+378\phi+210\phi^2)+\alpha_1(81+189\phi+105\phi^2)+\beta_1(46+111\phi+63\phi^2)$$

$$m_4=(39+94.5\phi+52.5\phi^2)+\alpha_1(18+40.5\phi+21\phi^2)+\beta_1(9.5+21\phi+10.5\phi^2)$$

$$m_5=(12+21\phi+10.5\phi^2)+\alpha_1(4.5+9\phi+5.25\phi^2)+\beta_1(2+4.5\phi+3\phi^2)$$

$$m_6=(39+94.5\phi+52.5\phi^2)+\alpha_1(21+54\phi+31.5\phi^2)+\beta_1(12.5+34.5\phi+21\phi^2)$$

$$m_7=(9+21\phi+10.5\phi^2)+\alpha_1(4.5+10.5\phi+5.25\phi^2)+\beta_1(2.5+6\phi+10.3\phi^2)$$

$$m_8=(468+882\phi+420\phi^2)+\alpha_1(360+672\phi+315\phi^2)+\beta_1(290+540\phi+252\phi^2)$$

$$m_9=(66+115.5\phi+52.5\phi^2)+\alpha_1(45+75\phi+31.5\phi^2)+\beta_1(32.5+52.5\phi+21\phi^2)$$

$$m_{10}=(12+21\phi+10.5\phi^2)+\alpha_1(7.5+12\phi+5.25\phi^2)+\beta_1(5+7.5\phi+3\phi^2)$$

$$[m_R]=\frac{\rho I_j}{210(1+\phi)^2}\begin{bmatrix} m_{11} & lm_{12} & -m_{11} & lm_{13} \\ & l^2m_{14} & -lm_{12} & -l^2m_{15} \\ & & m_{12} & -lm_{13} \\ symm & & & l^2m_{16} \end{bmatrix} \tag{16}$$

Where:

$$m_{12}=21+105\phi+\alpha_2(21-42\phi^2)+\beta_2(15-21\phi)+\gamma_2(10.5-12\phi)+\delta_2(7.5-7.5\phi)$$

$$m_{13}=21-105\phi-63\alpha_2\phi-\beta_2(6+42\phi)-\gamma_2(7.5+30\phi)-\delta_2(7.5+22.5\phi)$$

$$m_{14}=28-35\phi+70\phi^2+\alpha_2(7-7\phi+17.5\phi^2)+\beta_2(4-7\phi+7\phi^2)+\gamma_2(84-52.5\phi+26.25\phi^2)+\delta_2(78-42\phi+21\phi^2)$$

$$m_{15}=7+35\phi+35\phi^2+\alpha_2(3.5+17.5\phi+17.5\phi^2)+\beta_2(3-10.5\phi+10.5\phi^2)+\gamma_2(2.75-7\phi-7\phi^2)+\delta_2(2.5-5\phi+5\phi^2)$$

$$m_{16}=28+35\phi+70\phi^2+\alpha_2(21+42\phi-52.5\phi^2)+\beta_2(18-42\phi+42\phi^2)+\gamma_2(16.25+40\phi-35\phi^2)+\delta_2(15-37.5\phi+30\phi^2)$$

$$[G]=2[mR]$$

$$[k'']=\eta[K]$$

$$\left[k_g\right]=\frac{F_a}{30l\left(1+\phi\right)^2}\begin{bmatrix} k_{10} & lk_{11} & -k_{10} & lk_{11} \\ & l^2k_{12} & -lk_{11} & l^2k_{13} \\ & & k_{10} & -lk_{11} \\ symm & & & l^2k_{12} \end{bmatrix} \quad (17)$$

Where:

$k_{10}=36+60\phi+3\phi^2$

$k_{11}=3$

$k_{12}=4+5\phi+2.5\phi^2$

$k_{13}=1+5\phi+2.5\phi^2$

The equation of motion can be written as:

$$\begin{bmatrix}[m_x] & [0] \\ [0] & [m_y]\end{bmatrix}\{\ddot{q}\}+\omega\begin{bmatrix}[0] & [G] \\ -[G] & [0]\end{bmatrix}\{\dot{q}\}+\begin{bmatrix}[\eta_x] & [\eta_{xy}] \\ -[\eta_{xy}] & [\eta_Y]\end{bmatrix}\{\dot{q}\}+\begin{bmatrix}[K_x] & [K_{xy}] \\ [K_{xy}] & [K_Y]\end{bmatrix}\{q\}+\omega\begin{bmatrix}[0] & [\eta_r] \\ -[\eta_r] & [0]\end{bmatrix}\{\dot{q}\}=\begin{Bmatrix}R_e\left(\{f\}e^{i\omega t}\right) \\ \mathrm{Im}\left(\{f\}e^{i\omega t}\right)\end{Bmatrix} \quad (18)$$

4. Results and Discussion

A program is developed for calculating Natural frequencies and critical velocities and Natural modes for a cone-shaped model. The results obtained compared with those available in the literature. The properties and geometric dimensions of the shaft are:

E: Young modulus= 2.1011 N/m²

v : Poisson's ratio = 0.3

ρ : density = 7800 kg/m³

d1=0.1 m

d2=0.001 m

l= 16 m

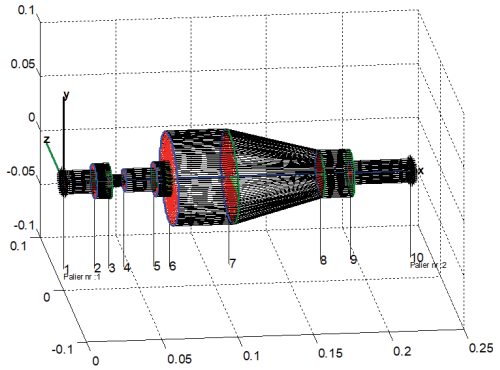

Figure 2: 3D rotor configuration.

The application of finite elements evaluates the natural frequencies of rotation of a discrete conical element in fourteen elements for a Timoshenko beam.

Discretization in fourteen conical elements:

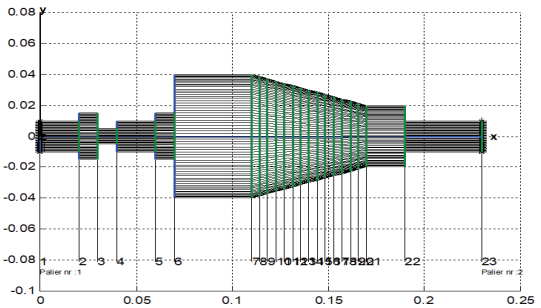

Figure 3: Rotor configuration discrete in fourteen elements.

Table 1: Natural values of the rotor system discretized in fourteen elements.

Number of own values	*DI Natural frequency [rpm]*	*DI Natural frequency (ZAHI et Al)[Hz]*	*DI Natural frequency (Genta et Al[23])[Hz]*
1	376	6,275	7.205
2	383	6,379	7.205
3	2010	33,497	34.955
4	2095	34,917	37.710
5	8732	145,527	X
6	8753	145,890	X
7	12884	214,733	X
8	12966	216,100	X
9	22665	377,750	X
10	22736	378,933	X

Table 1 presents data on the natural frequencies and damping coefficients for a conical element discretized into fourteen segments. This

discretization was accomplished using the Genta method of Timoshenko type, with a rotation speed of 12,000 rpm. Notably, the damping coefficients are reported as negative. Despite this unconventional observation, it's noted that negative damping coefficients typically indicate stable modes. This stability claim is further supported by the analysis presented in Figure 4, where the stability of the system is confirmed across various rotational speeds.

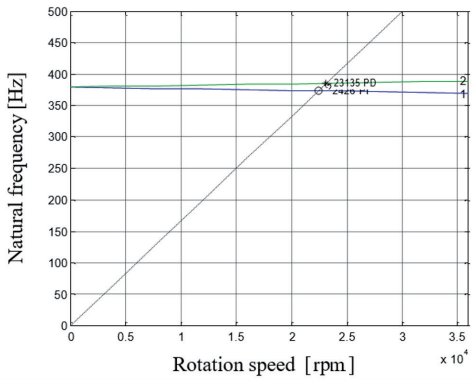

Figure 4: Campbell diagram.

From Campbell's diagram can determine the critical speed of Mode N °2:

Table 1: Critical speed.

Mode	Critical speed [rpm]
2	2.3135e +004

Figure 4 illustrates the variation of the bending fundamental frequency (ω) as a function of the rotating speed (Ω) of the tapered shaft. The gyroscopic effect inherent to rotating structures induces a precession motion. As the rotating speed increases, the direct modes increase, whereas the reverse modes decrease. The gyroscopic effect causes a coupling of orthogonal displacements to the axis of rotation, resulting in the separation of frequencies into two branches: backward precession mode and forward precession mode. In all cases, the forward modes increase with increasing rotating speed, while the backward modes decrease.

A Campbell diagram, also known as a Campbell plot or speed map, is a graphical representation used in rotor dynamics to analyze the critical speeds of a rotating system. It typically displays the rotor's natural frequencies (often referred to as critical speeds) as a function of rotational speed. Once you've located the curve corresponding to Mode N°2, find the intersection point between this curve and the rotor's rotational speed axis (typically represented in RPM or rad/s). This intersection point indicates the critical speed associated with Mode N°2.

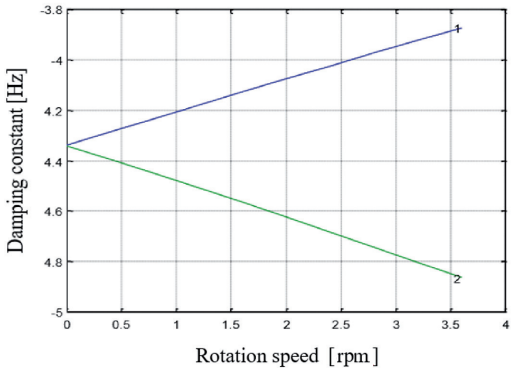

Figure 5: Stability diagram.

The stability diagram in Figure 5 confirms the stability of the rotor system irrespective of the rotational speed.

The stability diagram presented in Figure 5 likely plots the rotor's critical speeds or whirl frequencies against the rotational speed. The diagram may include curves indicating regions of stability and instability. Typically, regions below certain critical speeds or whirl frequencies indicate stable operation, while regions above indicate potential instability.

The first six modes and their frequency are calculated and presented in Figure 6

Figure 6 depicts the shape of the first six natural frequencies at 12,000 rpm. Natural frequencies correspond to specific mode shapes, which describe the spatial distribution of vibration within the system. For rotating machinery, mode shapes can include bending modes, torsional modes, and combinations thereof. In summary, the shape of the first natural frequencies at 12,000 rpm would depend on the specific characteristics of the system, including its geometry, material properties, and operating conditions. Analytical methods, numerical simulations, and experimental testing are typically employed to understand and characterize these frequencies accurately.

5. Conclusions

In conclusion, this study delves into the vibration analysis of rotors featuring a conical shaft through the application of finite element methods. The outcomes derived from numerical simulations are

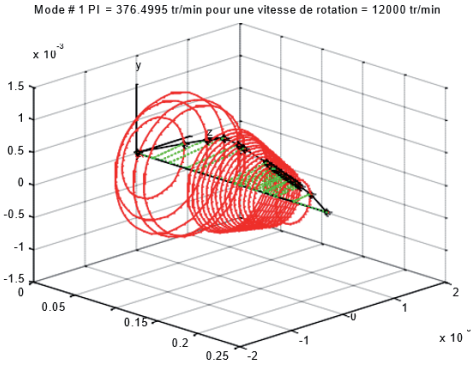

(a) Mode # PI = 376.4996 rpm
for rotation speed = 12000 rpm

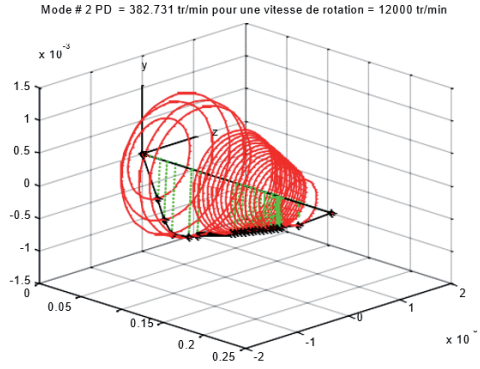

(b) Mode # 2PD = 382.731 rpm
for rotation speed = 12000 rpm

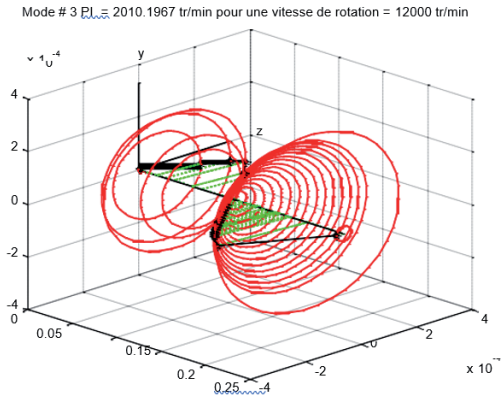

(c) Mode # 3PI = 2010.1967 rpm
for rotation speed = 12000 rpm

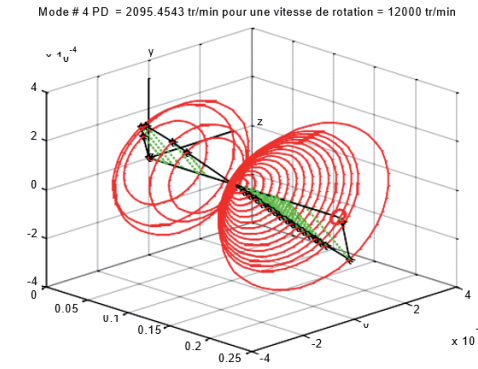

(d) Mode # 4PD = 2095.4643 rpm
for rotation speed = 12000 rpm

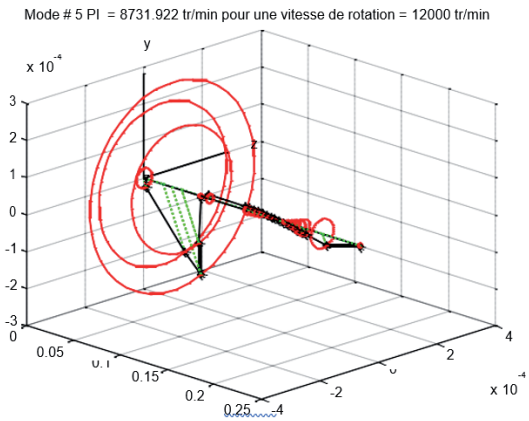

(e) Mode # 5PI = 8731.922 rpm
for rotation speed = 12000 rpm

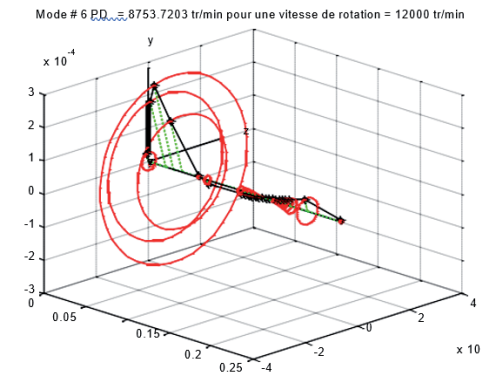

(f) Mode # 6PD = 8753.7203 rpm
for rotation speed = 12000 rpm

Figure 6: Shape of the first six element modes.

meticulously examined to underscore the necessity and benefits of incorporating conical finite element advancements.

– *Through numerical simulations, it is evident that the proposed conical finite element model offers highly accurate predictions regarding the dynamic behavior of rotors with a conical shaft.*

– *The observed increase in natural frequencies and critical speeds of the model underscores the inherent rigidity of the conical shaft. Furthermore, it's noteworthy that the reduction in natural frequency is contingent upon factors such as crack depth and location.*

Overall, the findings highlight the efficacy of employing conical finite element methodologies in understanding and predicting the dynamic characteristics of rotors with conical shafts, thereby enhancing our comprehension and ability to address related engineering challenges.

References

1. Nelson, H. D. and McVaugh, J. M. (1976). The Dynamics of Rotor-Bearing Systems Using Finite Elements. Journal of Engineering for Industry, 98(2), 593-600. https://doi.org/10.1115/1.3438942
2. Gash R. (1976). Vibrations of large turbo-Rotors in fluid film bearings on an Elastic Foundation. Journal of Sound and Vibration, (47)1,53-73. https://doi.org/10.1016/0022-460X(76)90407-7
3. Nelson, H. D. (1980). A Finite Rotating Shaft Element Using Timoshenko Beam Theory. journal of mechanical design. 102(4), 793-803. https://doi.org/10.1115/1.3254824.
4. Ozguven, H.N. and Ozkan, Z.L. (1984). Whirl speeds and Unbalance Responses of multi-bearing Rotor using Finite Element. Journal of Vibration Acoustics Stress, and Reliability in Design. 106(1), 72-79. https://doi.org/10.1115/1.3269158.
5. Ku, D. M. (1998). Finite element analysis of whirl speeds for rotor-bearing systems with internal damping. Mechanical Systems and Signal Processing. 12(5), 599-610. https://doi.org/10.1006/mssp.1998.0159.
6. Rouch, K. E. and Kao, J. S. (1979). A tapered beam finite element for rotor dynamics analysis. J. of Sound and Vibration, 66(1), 119–140. https://doi.org/10.1016/0022-460X(79)90607-2.
7. Archer, J.S. (2012). Consistent matrix formulation for Structural Analysis Using Finite Element Techniques. AIAA Journal, 3(10),1910-1918. https://doi.org/10.2514/3.3279.
8. Greenhill, L.M., Bickford, W.B. and Nelson, H.D. (1985). A conical beam finite element for rotor dynamics analysis. Journal of Sound and Vibration, 107(4), 421-430. https://doi.org/10.1115/1.3269283.
9. Jia, Z., Yang, Y., Zheng, Q. and Deng, W. (2022). Dynamic analysis of jeffcott rotor under uncertainty based on chebyshev convex method, Mechanical Systems and Signal Processing, 167 Part B, 108603. . https://doi.org/10.1016/j.ymssp.2021.108603.
10. Numanoğlu, H.M., Ersoy, H., Akgöz, B., and Civalek, Ö. (2022). A new eigenvalue problem solver for thermo-mechanical vibration of Timoshenko nanobeams by an innovative nonlocal finite element method. Mathematical Methods in the Applied Sciences, 45(5), 2592–2614. https://doi.org/10.1002/mma.7942.
11. Ahmed, O., El-Sayed, T. and Sayed, H. (2023). Finite element analyses of rotor/bearing system using second-order journal bearings stiffness and damping coefficients, Journal of Vibration and Control, 0(0), 1–24. https://doi.org/10.1177/10775463231204388.
12. Ghayesh, M. H., Ghazavi, M. R. and Khadem, S. E. (2010). Non-linear vibration and stability analysis of an axially moving rotor in sub-critical transporting speed range. Structural Engineering and Mechanics, 34(4), 507-523. https://doi.org/10.12989/sem.2010.34.4.507.
13. Jeong S. H. (2014). Krylov subspace-based model order reduction for Campbell diagram analysis of large- scale rotor dynamic systems. Structural Engineering and Mechanics, 50(1), 019-036. https://doi.org/10.12989/sem.2014.50.1.019.
14. Fatehi, M. R., Ghanbarzadeh, A., Moradi, S. and Hajnayeb, A. (2018). Global sensitivity analysis improvement of rotor-bearing system based on the Genetic Based Latine Hypercube Sampling (GBLHS) method. Structural Engineering and Mechanics, 68(5), 549-561. https://doi.org/10.12989/sem.2018.68.5.549.
15. Saldarriaga, M. V., Mahfoud, J., Steffen, V. Jr. and Hagopian, J. D. (2009). Adaptive balancing of highly flexible rotors by using artificial neural networks. Smart Structures and Systems, 5(5), 507-515. https://doi.org/10.12989/sss.2009.5.5.507.
16. Liu, P., Chen, A. Y., Huang, Y. N., Han, J. Y., Lai, J. S., Kang, S. Ch., Wu, T. H., Wen, M. Ch. and Tsai, M.H. (2014). A review of rotorcraft Unmanned Aerial Vehicle (UAV) developments and applications in civil engineering. Smart Structures and Systems, 13(6), 1065-1094. https://doi.org/10.12989/sss.2014.13.6.1065.
17. Muñoz-Abella, B., Ruiz-Fuentes, A., Rubio, P., Montero, L. and Rubio, L. (2020). Cracked rotor diagnosis by means of frequency spectrum and artificial neural networks. Smart Structures and Systems, 25(4), 459-469. https://doi.org/10.12989/sss.2020.25.4.459.
18. Matthew, G. R., Nikola S. and Ian K. S. (2020). The Influence of Rotor Geometry on Power Transfer Between Rotors in Gerotor-Type Screw Compressors. journal of mechanical design, 142(7), 073501. https://doi.org/10.1115/1.4045508.

19. Vinod Kumar, N., Prathapanayaka, R., Jai Maruthi, R., Swaroop, S. (2021). 3D Finite Element Rotor Dynamic Analysis of Turbine Test Rig Rotor-Shaft Systems. In: Rao, J.S., Arun Kumar, V., Jana, S. (eds) Proceedings of the 6th National Symposium on Rotor Dynamics. Lecture Notes in Mechanical Engineering. Springer, October, Singapore. https://doi.org/10.1007/978-981-15-5701-9_2.
20. Shravankumar, C., Jegadeesan, K., Rao, T.V.V.L.N. (2021). Analysis of Rotor Supported in Double-Layer Porous Journal Bearing with Gyroscopic Effects. In: Rao, J.S., Arun Kumar, V., Jana, S. (eds) Proceedings of the 6th National Symposium on Rotor Dynamics. Lecture Notes in Mechanical Engineering. Springer, October, Singapore. https://doi.org/10.1007/978-981-15-5701-9_6.
21. Gayen, D., Tiwari, R., Chakraborty, D. (2021). Thermo-Mechanical Analysis of a Rotor-Bearing System Having a Functionally Graded Shaft with Transverse Breathing Cracks. In: Rao, J.S., Arun Kumar, V., Jana, S. (eds) Proceedings of the 6th National Symposium on Rotor Dynamics. Lecture Notes in Mechanical Engineering. Springer, October, Singapore. https://doi.org/10.1007/978-981-15-5701-9_8.
22. Lalanne, M. and Ferraris, G. (1998). Rotor-dynamics Prediction in Engineering. 1st edition, Wiley, New York.
23. Genta, G., & Gugliotta, A. (1988). A conical element for finite element rotor dynamics. Journal of Sound and Vibration, 120(1), 175-182.
24. Rachid, Z., Abderahmane, S., Abdelmadjid, M., Noureddine, Z., & Kaddour, R. (2023). Dynamic analysis of a rotating tapered composite Timoshenko shaft. Steel and Composite Structures, 48(4), 429.
25. Zahi, R., Sahli, A., Kaci, D., Bourada, F., Tounsi, A., & Ghazwani, M. H. (2023). Study and analysis of a tapered shaft in composite materials with variable speed of rotation. Structural Engineering and Mechanics, 87(2), 191-200.